

Karyotype evolution and acquisition of *FLT3* or *RAS* pathway alterations drive progression of myelodysplastic syndrome to acute myeloid leukemia

Manja Meggendorfer,^{1*} Andreia de Albuquerque,^{1*} Niroshan Nadarajah,¹ Tamara Alpermann,¹ Wolfgang Kern,¹ Kimberly Steuer,¹ Karolína Perglerová,² Claudia Haferlach,¹ Susanne Schmittger,¹ and Torsten Haferlach¹

**contributed equally to this work*

¹MLL Munich Leukemia Laboratory, Munich, Germany; and ²MLL2 s.r.o., Praha, Czech Republic

Acknowledgments: we thank all clinicians for sending samples to our laboratory for diagnostic purposes and for providing clinical information and follow-up data. In addition, we would like to thank all the co-workers at the MLL Munich Leukemia Laboratory, who contributed to sequencing analyses in this study.

Correspondence: torsten.haferlach@mll.com

doi:10.3324/haematol.2015.127985

SUPPLEMENTAL INFORMATION

Karyotype evolution and acquisition of *FLT3* or *RAS* pathway alterations drive progression of myelodysplastic syndrome to acute myeloid leukemia

1. Patients and methods

1.1 Patient cohorts

A total of 38 patients were analyzed both at diagnosis of MDS and later at progression to s-AML following MDS. Clinical data, like sex, age, % blasts, karyotype, and time to diagnosis of s-AML are given in table S1. Samples were referred to our laboratory between October 2005 and November 2012 for diagnostic assessment. Diagnosis was performed on bone marrow smears according to standard World Health Organization (WHO) criteria.¹ Patients were diagnosed as: RARS (n=2), RCMD (n=3), RCMD-RS (n=8), RAEB-1 (n=12), RAEB-2 (n=12) and MDS with isolated 5q deletion (n=1).

For comparison a subgroup of the MDS cohort previously published in Haferlach *et al.*² was taken. From this cohort, patients showing a transformation to s-AML were excluded (n=78) and taken as separate control cohort. Since the median time to transformation was 18 months in the MDS/s-AML cohort, all cases with follow-up less than 18 months were also excluded from this control cohort. The cohort was matched to WHO diagnosis of the present MDS/s-AML cohort, resulting in the final MDS control cohort of 494 patients.

All patients gave their written informed consent for scientific evaluations. The study design adhered to the tenets of the Declaration of Helsinki and was approved by our institutional review board before its initiation.

1.2 Cytomorphology

In all cases bone marrow smears underwent May Giemsa Gruenwald staining. For cytomorphology, 200 nucleated cells were counted in the bone marrow. Cytochemistry was performed for myeloperoxidase (MPO) and non-specific esterase (NSE), and iron staining was done for detection of ring sideroblasts in cases with increased erythropoiesis or anemia. Classification of the disease entities and dysplasia was rated according to WHO criteria.¹

1.3 Cytogenetics and fluorescence in situ hybridization (FISH)

Chromosome banding analysis was performed in all cases after short-term culture. Karyotypes were analyzed after G-banding and described according to the International System for Human Cytogenetic Nomenclature.³ Interphase FISH was applied with probes for the centromeric region of chromosome 8 (CEP8 DNA probe kit, ABBOTT, Wiesbaden, Germany). All karyotypes are given in table S1.

Table S1 – Clinical characterization of patients

Patient	MDS diagnosis	Female (F), Male (M)	Age (years)	% Blasts (MDS)	% Blasts (AML)	MDS karyotype	s-AML karyotype	Time to progression (months)
1	RARS	M	60	1	8.5	46,XY[20]	46,XY[20]	4
2	RAEB-2	F	82.9	14.5	77	46,XX[20]	47,XX,+4[6] 46,XX[9]	35
3	RAEB-1	F	76.4	6.5	63	46,XX[20]	46,XX,del(5)(q22q34),del(7)(q22q36)[9] 46,XX[1]	21
4	RAEB-1	M	62.4	8	44	46,XY,t(1;3)(p36;q21)[15]	46,XY,t(1;3)(p36;q21)[17]	10
5	RAEB-2	M	63.8	10.5	26	46,XY[16]	46,XY[20]	73
6	RCMD-RS	F	66.5	2.5	74	46,XX[25]	46,XX[21]	6
7	RAEB-1	M	76.7	8	82	45,X,-Y[19] 46,XY[1]	45,X,-Y[20]	5
8	RAEB-2	F	77.3	17.5	34	48,XX,+1,del(5)(q14q34),+11[20] 46,XX[1]	48,XX,+1,del(5)(q14q34),+11[10] 49,XX,+1,del(5)(q14q34),+11,+22[3] 50,XX,+1,del(5)(q14q34),+11,+r(11)(p13q14),+22[7]	22
9	RAEB-2	M	78.1	10	33	47,XY,+19[8] 47,XY,+8[4] 46,XY [8]	46,XY,-7,del(12)(p11p13),+19[17] 46,XY [4]	34
10	RAEB-2	M	67.1	15	22	46,XY[18]	46,XY[20]	9
11	RCMD-RS	M	60.9	4.5	20	46,XY,del(20)(q11)[13] 46,XY[4]	46,XY,del(20)(q11q13)[9] 47,XY,+8,del(20)(q11q13)[8] 45,XY,der(16;17)(p10;q10),del(20)(q11q13)[13]	50
12	RAEB-2	M	71.7	16	30	46,XY[20]	48,XY,+1,der(1;13)(q10;q10),+i(5)(p10),+8[9] 46,XY[11]	11
13	RCMD-RS	M	76.8	3	20.5	46,XY[20]	46,XY[20]	8
14	RAEB-1	F	72.7	8.5	34.5	46,XX[17]	46,XX[17]	21
15	RAEB-1	M	59.1	6.5	27.5	46,XY[20]	46,XY.ish del(4)(q24q24)(TET2-)[11] 48,XY,+8,+20.ish del(4)(q24q24)(TET2-)[1] 49,XY,+5,+8,+20.ish del(4)(q24q24)(TET2-)[2] 50,XY,+5,+8,+15,+20.ish del(4)(q24q24)(TET2-)[4]	55
16	RAEB-1	M	74.3	9	49.5	47,XY,+13[8] 48,XY,+13,+13[11] 46,XY[1]	47,XY,+13[5] 48,XY,+13,+13[2] 46,XY,i(17)(q10)[3] 47,XY,+13,i(17)(q10)[2]	17
17	RAEB-2	M	61.8	12	45	46,XY[20]	46,XY[20]	33
18	RARS	M	69.4	5	14	46,XY[20]	47,XY,+8[1]* 46,XY[19]	2
19	RCMD-RS	M	76.3	4.5	21	46,XX,t(2;3)(p21;q26)[19]	46,XX,t(2;3)(p21;q26)[8] 46,XX[12]	27

20	RAEB-2	M	72	13	57.5	47,XY,+8 [18] 46,XY[2]	47,XY,+8 [16] 46,XY[4]	21
21	RCMD	M	79.4	4.5	86	47,XY,+8[19] 46,XY[3]	47,XY,+8[20]	9
22	RAEB-1	F	68.6	5	61	47,XX,+8[17] 46,XX[3]	47,XX,+8[19] 46,XX[1]	19
23	RCMD-RS	F	64.7	3	74	46,XX,del(9)(q22q34)[2] 46,XX[18]	46,XX,del(9)(q22q34)[20] 46,XX[1]	8
24	RAEB-1	M	72.3	9	67.5	46,XY[20]	46,XY[20]	18
25	RAEB-1	M	69.3	9.5	56	46,XY[20]	45,XY,t(3;21)(q26;q22),-7[5] 46,XY[7]	27
26	RCMD	M	68.1	4	27.5	46,XY[20]	46,XY[20]	31
27	RAEB-2	M	58.8	13	61	46,XY[20]	46,XY[20]	19
28	RAEB-2	M	63.3	10	45.5	46,XY[20]	46,XY[22]	11
29	RCMD	M	69.6	4.5	59	46,XY[20]	45,X,-Y[11] 46,X,-Y,+20[5] 46,XY[5]	20
30	RAEB-1	F	62.3	9	21.5	46,XX[20]	46,XX[20]	12
31	RAEB-2	F	85.7	18	88	46,XX[20]	46,XX[20]	10
32	5q- Syndrome	F	82.3	3	50	46,XX,del(5)(q14q34)[7] 46,XX[13]	46,XX,del(5)(q14q34)[17] 46,XX[3]	29
33	RCMD-RS	M	70.8	2	74	46,XY[20]	46,XY[20]	7
34	RCMD-RS	M	80.7	4.5	28.5	46,XY,del(20)(q11q13),t(22;22)(q11;q13)[16] 46,XY[1]	46,XY,del(20)(q11q13),t(22;22)(q11;q13)[20]	19
35	RAEB-2	F	74.9	10.5	68	46,XX[20]	46,XX[20]	20
36	RCMD-RS	M	78.9	0	33	46,XY[21]	46,XY[20]	8
37	RAEB-1	M	68.5	6	89	47,XY,+8 [10] 46,XY [10]	47,XY,der(3)t(3;3)(p26;q24),+8,der(16)t(3;16)(?;q24), der(17)t(16;17)(q24;p11)[13]	3
38	RAEB-1	M	75.4	7	83	46,XY[22]	46,XY,del(3)(q11q26)[2] 47,XY,del(3)(q11q26),+8[4] 46,XY[10]	10

* clonality of trisomy 8 was proven by FISH on interphase nuclei

1.4 Isolation of nucleic acid

DNA or RNA from fresh bone marrow cells was isolated after Ficoll separation of mononucleated cells. DNA was isolated using the DSP DNA Midi Kit and the QIASymphony instrument (Qiagen, Hilden, Germany). RNA was isolated using the MagNa Pure LC system with the corresponding mRNA HS Kit (Roche Applied Science, Mannheim, Germany). RNA was reverse transcribed with 500 U SuperScript II Reverse Transcriptase enzyme (Invitrogen, Carlsbad, CA) in a 50 µl reaction using random hexamers as primers.

1.5 Targeted library preparation and next generation sequencing

The primer library consisted of oligonucleotides for successful amplification of 389 amplicons including exon/intron boundaries. The amplicons ranged from 150 – 240 bp (median 205 bp), representing a total target sequence of 78.15 kb. The median coverage for all 76 analyzed patients was 7363 reads (3684 for read 1 and 3679 for read 2) and the detection limit for variants was 3%.

The template library was prepared following the manufacturers protocol (RainDance Technologies, Billerica, MA). Briefly, for each patient, 2.2 µg genomic sheared DNA was combined with a PCR reaction mix without oligonucleotide primer molecules. This reaction mastermix and the myeloid primer library were loaded separately into the ThunderStorm instrument (RainDance Technologies) where droplets containing one myeloid primer library per droplet were generated for PCR amplification. Next, emulsion PCR droplets were broken releasing the amplicons for purification and quantification. Barcode indices and suitable MiSeq adaptor sequences were added using a second-round PCR step. After amplification and purification, samples were quantified and equal amounts of each tagged library were pooled for cluster generation and sequencing. PhiX control libraries (Illumina, San Diego, CA) were added (1.5% final concentration) to the pooled NGS library and used to increase the diversity of base calling during sequencing. Libraries were sequenced on the MiSeq sequencing-by-synthesis benchtop sequencer according to the manufacturer's protocol (Illumina). MiSeq v2 (500-cycles) reagent cartridges (Illumina) were used to sequence libraries with paired-end (2 x 251). All steps were performed according to the instructions of the manufacturers. The quality of the sequence run was monitored by the Sequencing Analysis Viewer (SAV, Illumina). Data was automatically demultiplexed on the MiSeq instrument and corresponding zipped FASTQ files were generated per barcode index. The zipped FASTQ files were further processed using the Sequence Pilot software version 4.1.1 Build 510 (JSI Medical Systems, Kippenheim, Germany) for alignment and variant calling. If a mutation was detected in any s-AML sample, that was not present during MDS stage, the sequence was manually analyzed and sequenced by using the 454 platform to ensure that no mutations with low mutation load were missed.

1.6 Next generation sequencing of *RUNX1* and *ZRSR2*

Next generation deep-sequencing of the *RUNX1* and *ZRSR2* gene was performed using the 454 GS FLX amplicon chemistry (Roche Applied Science) as previously described.⁴

1.7 Next generation sequencing of *SMC1A*, *SMC3*, *RAD21*, *STAG2*, and *SETBP1*

Next generation sequencing of *SMC1A*, *SMC3*, *RAD21*, *STAG2*, and *SETBP1* was performed using the Fluidigm Access Array microfluidic chip system (Fluidigm, San Francisco, CA). These chips feature the combination of 48 samples with primer groups for PCR amplification in individual reaction chambers. Following PCR, the samples of one Access Array chip were barcoded in a second PCR step and then pooled. The pool was purified using Ampure Beads (Beckman Coulter, Brea, CA) to remove primer-dimer products and went on a MiSeq Instrument together with a 1.5% PhiX spike (Illumina, San Diego, CA). MiSeq v3 (600-cycles) reagent cartridges (Illumina) were used to sequence libraries with paired-end (2 x 301). All steps were performed according to the instructions of the manufacturers.

1.8 PCR for detection of *MLL*-PTD and *FLT3*-ITD

MLL-PTD was analyzed with a quantitative PCR assay, *FLT3*-ITD was analyzed by gene scan, both described methodically previously.^{5,6} Detection limit for *FLT3*-ITD was 5%.

1.9 Statistical analyses

Dichotomous variables were compared between different groups using the χ^2 -test or Fisher's exact test. Odds ratios were estimated by the Mantel-Haenszel test and the 95% confidence intervals were given. Results were considered significant at $p < 0.05$; the reported p -values are two-sided. Adjustment for multiple testing was not done. Statistical analyses were performed using SPSS version 19.0 (IBM Corporation, Armonk, NY).

2. Analyses of mutational loads of mutations at MDS and s-AML stages - clonal evolution

Next generation sequencing allows to investigate variant allele frequencies. In the total cohort of 38 paired samples (n=76) the allele frequencies were analyzed. However, the major changes between MDS and s-AML stages were gain or loss of mutation. The persisting mutations remained quite stable with only single exceptions. The allele frequencies for all patients and genes that were either at MDS or s-AML or both stages mutated are given in table S2.

Table S2 - Variant allele frequencies for all mutations identified either at MDS, s-AML, or both stages

Patient	mutated gene	load [%] MDS	load [%] s-AML	Patient	mutated gene	load [%] MDS	load [%] s-AML	Patient	mutated gene	load [%] MDS	load [%] s-AML
1	<i>CBL</i>	46	47	11	<i>CBL</i>	0	9	17	<i>GATA2</i>	39	49
	<i>SF3B1</i>	47	50		<i>IDH2</i>	50	48		<i>JAK2</i>	0	4
	<i>TET2</i>	96	97		<i>SRSF2</i>	32	37		<i>SRSF2</i>	45	49
	<i>SMC1A</i>	0	81		<i>NPM1</i>	0	9		<i>ASXL1</i>	8	0
2	<i>SMC3</i>	0	37	12	<i>SRSF2</i>	27	48	18	<i>ASXL1</i>	39	42
	<i>SRSF2</i>	48	62		<i>SRSF2</i>	42	45		<i>IDH2</i>	49	47
	<i>TET2</i>	36	44		<i>TET2</i>	37	35		<i>SRSF2</i>	47	49
	<i>TET2</i>	46	41		<i>TET2</i>	4	0		<i>STAG2</i>	31	18
3	<i>U2AF1</i>	0	21	13	<i>DNMT3A</i>	0	9	19	<i>BRAF</i>	40	44
	<i>KRAS</i>	0	46		<i>DNMT3A</i>	42	50		<i>FLT3(TKD)</i>	40	34
	<i>NRAS</i>	16	0		<i>RUNX1</i>	18	16		<i>SF3B1</i>	43	44
	<i>RUNX1</i>	45	0		<i>RUNX1</i>	0	25		<i>ASXL1</i>	43	43
4	<i>RUNX1</i>	0	36	14	<i>SF3B1</i>	0	29	20	<i>ETV6</i>	45	44
	<i>NRAS</i>	9	40		<i>SF3B1</i>	40	40		<i>EZH2</i>	47	48
	<i>SF3B1</i>	46	46		<i>ASXL1</i>	39	46		<i>EZH2</i>	45	47
	<i>RUNX1</i>	44	49		<i>BCOR</i>	6	29		<i>FLT3(TKD)</i>	0	32
5	<i>SETBP1</i>	50	53	15	<i>KIT</i>	4	0	21	<i>PHF6</i>	0	7
	<i>SRSF2</i>	51	46		<i>KIT</i>	39	50		<i>RUNX1</i>	44	44
	<i>TET2</i>	45	48		<i>NRAS</i>	39	0		<i>ASXL1</i>	28	31
	<i>TET2</i>	44	48		<i>NRAS</i>	6	0		<i>TET2</i>	44	45
6	<i>RUNX1</i>	2	100	16	<i>RUNX1</i>	41	50	22	<i>TET2</i>	44	47
	<i>SF3B1</i>	41	45		<i>U2AF1</i>	49	49		<i>NRAS</i>	0	50
	<i>TET2</i>	3	0		<i>ASXL1</i>	0	22		<i>RUNX1</i>	0	4
	<i>TET2</i>	50	49		<i>KRAS</i>	0	27		<i>STAG2</i>	60	91
7	<i>KRAS</i>	4	0	17	<i>TET2</i>	88	84	23	<i>TET2</i>	90	95
	<i>NPM1</i>	46	46		<i>ZRSR2</i>	95	95		<i>ASXL1</i>	49	35
	<i>WT1</i>	44	64		<i>ASXL1</i>	33	35		<i>ASXL1</i>	52	47
	<i>WT1</i>	20	0		<i>CBL</i>	43	42		<i>DNMT3A</i>	46	40
8	<i>TP53</i>	42	44	18	<i>CBL</i>	42	55	19	<i>IDH2</i>	47	43
	<i>TP53</i>	36	53		<i>ETV6</i>	47	45		<i>SRSF2</i>	46	32
	<i>TP53</i>	42	44		<i>NRAS</i>	4	0		<i>DNMT3A</i>	71	88
	<i>TP53</i>	36	53		<i>NRAS</i>	45	47		<i>KRAS</i>	0	6
9	<i>SRSF2</i>	43	40	19	<i>SRSF2</i>	42	45	20	<i>NPM1</i>	0	38
	<i>ASXL1</i>	43	44		<i>SETBP1</i>	45	47		<i>NRAS</i>	0	34
	<i>IDH2</i>	46	46		<i>SRSF2</i>	42	45		<i>SF3B1</i>	33	44
	<i>STAG2</i>	0	87								

Patient	mutated gene	load [%] MDS	load [%] s-AML
24	<i>ASXL1</i>	27	32
	<i>NRAS</i>	0	27
		0	5
	<i>RUNX1</i>	19	42
	<i>SRSF2</i>	40	49
	<i>STAG2</i>	42	82
		22	47
	<i>TET2</i>	20	0
		43	46
25	<i>ASXL1</i>	44	44
	<i>PHF6</i>	0	5
	<i>TET2</i>	43	45
		44	45
	<i>U2AF1</i>	47	44
26	<i>ASXL1</i>	25	30
	<i>NRAS</i>	0	6
	<i>RUNX1</i>	0	47
	<i>SRSF2</i>	45	45
27	<i>IDH1</i>	43	48
	<i>PHF6</i>	15	10
	<i>SF3B1</i>	0	5
	<i>U2AF1</i>	6	0
28	<i>ASXL1</i>	25	34
	<i>DNMT3A</i>	4	0
	<i>IDH2</i>	25	48
	<i>SRSF2</i>	3	35
	<i>STAG2</i>	28	75
29	<i>ASXL1</i>	0	8
	<i>CBL</i>	35	54
		0	37
	<i>JAK2</i>	24	0
	<i>TET2</i>	75	93
		20	0
	<i>ZRSR2</i>	96	93

Patient	mutated gene	load [%] MDS	load [%] s-AML
30	<i>ASXL1</i>	26	49
	<i>CBL</i>	20	0
	<i>NRAS</i>	0	44
31	<i>ASXL1</i>	0	45
	<i>IDH2</i>	45	45
	<i>RUNX1</i>	14	74
	<i>SRSF2</i>	54	43
32	<i>TP53</i>	11	75
33	<i>ETV6</i>	33	33
	<i>FLT3(TKD)</i>	0	5
	<i>NRAS</i>	0	6
	<i>RUNX1</i>	38	42
	<i>SF3B1</i>	42	40
	<i>SRSF2</i>	38	41
34	<i>GATA2</i>	3	74
	<i>KRAS</i>	0	24
	<i>NRAS</i>	0	19
	<i>RUNX1</i>	4	0
	<i>SRSF2</i>	34	39
35	<i>ASXL1</i>	27	26
	<i>BCOR</i>	45	44
	<i>KRAS</i>	0	5
	<i>NRAS</i>	0	33
	<i>RUNX1</i>	37	38
36	<i>SRSF2</i>	37	34
	<i>DNMT3A</i>	47	48
	<i>IDH2</i>	50	47
	<i>SRSF2</i>	47	47
37	<i>KRAS</i>	0	45
	<i>TET2</i>	32	44
	<i>TP53</i>	0	75
	<i>U2AF1</i>	42	45
38	<i>SF3B1</i>	5	0
	<i>SRSF2</i>	40	46
	<i>TET2</i>	44	48
		45	48

3. Comparison of MDS/s-AML cases at MDS stage with independent MDS/s-AML control cohort

To validate our findings, we defined cases of the previously published well characterized MDS cohort,² that showed transformation to s-AML (n=78) and compared these MDS cases with the MDS cases of the present cohort, regarding cytogenetics and molecular mutations. There were no significant differences in mutation frequencies. The associations as well the numbers of cases with mutations are given in figure S3. These results validate that the detected increased mutation frequencies in *ASXL1*, *CBL*, *GATA2*, *IDH2*, *NRAS*, *RUNX1*, and *SRSF2* relative to MDS cases without transformation, impact the disease progression to s-AML.

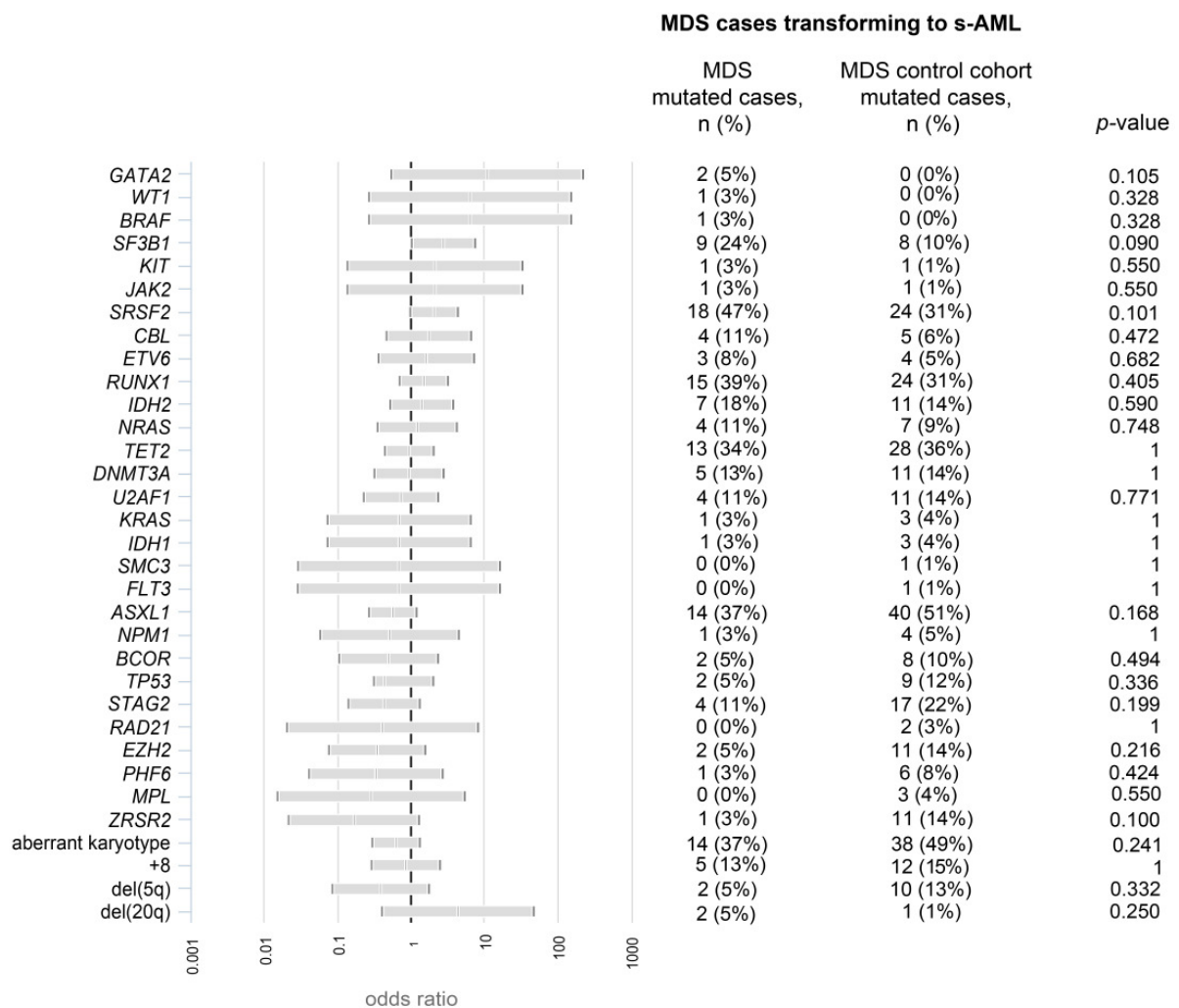


Figure S3 – Associations of aberrations to the MDS or the MDS control cohort (all patients show s-AML transformation) are depicted by the odds ratio of MDS/MDS control cohort, the 95% confidence interval is given. Odds ratio of 1 indicates that mutation frequencies are comparable in both cohorts. Numbers of cases with respective mutations and karyotype aberrations as well as p-values are given in the table beside.

REFERENCES

1. Swerdlow SH, Campo E, Harris NL, Jaffe ES, Pileri SA, Stein H et al. WHO Classification of Tumours of Haematopoietic and Lymphoid Tissues, 4th ed. Lyon: International Agency for Research on Cancer (IARC), 2008.
2. Haferlach T, Nagata Y, Grossmann V, et al. Landscape of Genetic Lesions in 944 Patients with Myelodysplastic Syndromes. *Leukemia*. 2014;28(2):241-247.
3. Shaffer LG, McGowan-Jordan J, Schmid M. ISCN 2013: an international system for human cytogenetic nomenclature. Basel, New York: Karger, 2013.
4. Kohlmann A, Klein HU, Weissmann S, et al. The Interlaboratory ROBustness of Next-generation sequencing (IRON) study: a deep sequencing investigation of TET2, CBL and KRAS mutations by an international consortium involving 10 laboratories. *Leukemia*. 2011;25(12):1840-1848.
5. Schnittger S, Kinkelin U, Schoch C, et al. Screening for MLL tandem duplication in 387 unselected patients with AML identify a prognostically unfavorable subset of AML. *Leukemia*. 2000;14(5):796-804.
6. Schnittger S, Schoch C, Kern W, et al. FLT3 length mutations in AML: Correlation to cytogenetics, FAB- subtype, and prognosis in 652 patients. *Blood*. 2000;96:826a.